Crystal structure of a cyanobacterial phytochrome response regulator

YOUNG JUN IM,[1] SEONG-HWAN RHO,[1] CHUNG-MO PARK,[2] SONG-SOOK YANG,[2] JEONG-GU KANG,[2] JAE YOUNG LEE,[3] PILL-SOON SONG,[1,2,4] AND SOO HYUN EOM[1]

[1]Department of Life Science, Kwangju Institute of Science and Technology, Kwangju 500-712, Korea
[2]Kumho Life and Environmental Science Laboratory, 1 Oryong-dong, Buk-gu, Kwangju 500-712, Korea
[3]School of Chemistry, College of Natural Sciences, Seoul National University, Seoul 151-742, Korea
[4]Department of Chemistry, University of Nebraska, Lincoln, Nebraska 68588, USA

(RECEIVED September 24, 2001; FINAL REVISION November 26, 2001; ACCEPTED November 30, 2001)

Abstract

The two-component signal transduction pathway widespread in prokaryotes, fungi, molds, and some plants involves an elaborate phosphorelay cascade. Rcp1 is the phosphate receiver module in a two-component system controlling the light response of cyanobacteria *Synechocystis* sp. via cyanobacterial phytochrome Cph1, which recognizes Rcp1 and transfers its phosphoryl group to an aspartate residue in response to light. Here we describe the crystal structure of Rcp1 refined to a crystallographic *R-factor* of 18.8% at a resolution of 1.9 Å. The structure reveals a tightly associated homodimer with monomers comprised of doubly wound five-stranded parallel β-sheets forming a single-domain protein homologous with the N-terminal activator domain of other response regulators (e.g., chemotaxis protein CheY). The three-dimensional structure of Rcp1 appears consistent with the conserved activation mechanism of phosphate receiver proteins, although in this case, the C-terminal half of its regulatory domain, which undergoes structural changes upon phosphorylation, contributes to the dimerization interface. The involvement of the residues undergoing phosphorylation-induced conformational changes at the dimeric interface suggests that dimerization of Rcp1 may be regulated by phosphorylation, which could affect the interaction of Rcp1 with downstream target molecules.

Keywords: Response regulator; two-component system; cyanobacterial phytochrome; Rcp1

A complex network of interacting proteins regulates bacterial responses to environmental conditions, with the most predominant interactions being generated by members of the two-component systems (Parkinson 1993). In this system a sensor kinase interprets specific signals, resulting in an autophosphorylation reaction in which a phosphate from ATP is transferred to a histidine residue on the kinase (Ninfa and Magasanik 1986). The phosphoryl group is then donated to an aspartate residue on the response regulator, which in turn, serves to modulate downstream signal transduction (Stock et al. 1989; Parkinson and Kofoid 1992). It has been estimated that *Escherichia coli* contains 32 response regulators, which govern various cellular responses to stress and environmental change (West and Stock 2001). Two-component systems not only show great diversity in signal specificity and are widely spread throughout more than 30 prokaryotic genera (Volz 1993), but have also been found in such eukaryotes as *Arabidopsis thaliana* (Chang et al. 1993), *Saccharomyces cereviae* (Ota and Varshavsky 1993; Maeda et al. 1994), and *Neurospora crassa* (Alex et al. 1996): a plant, a yeast, and a fungus, respectively.

The cyanobacterial phytochrome Cph1 found in *Synechocystis* PCC6803 is a spectrally active histidine kinase that mediates red/far-red reversible phosphorylation of a small response regulator, Rcp1 (Yeh et al. 1997). The *rcp1* gene encodes a 147-amino acid protein related to the CheY su-

Reprint requests to: Soo Hyun Eom, Department of Life Science, Kwangju Institute of Science and Technology, Kwangju 500-712, Korea; e-mail: eom@kjist.ac.kr; fax: 82-62-970-2548.

Article and publication are at http://www.proteinscience.org/cgi/doi/10.1110/ps.39102.

perfamily of bacterial response regulators, which contain aspartate kinase receiver modules (Yeh et al. 1997). The *cph1* sequence encodes a putative protein with an N-terminal chromophore domain resembling that of higher plant phytochromes and a C-terminal domain resembling the histidine-kinase domain of the bacterial two-component family (Lamparter et al. 1997; Park et al. 2000). Cph1 exists in two interconvertible forms, termed Pr (red-light absorbing form) and Pfr (far-red-light absorbing form). Red light converts Pr to Pfr and far-red light converts Pfr back to Pr. In far-red light or in the dark, Cph1 (Pr form) phosphorylates itself at a histidine residue, then transfers the phosphate group to Rcp1, putting Rcp1 in a signaling state able to regulate an unknown response. In red light, Cph1 (Pfr form) is inactive, and unphosphorylated Rcp1 exists in the opposite signaling state (Yeh et al. 1997). The exact role of Rcp1 and its downstream signal transduction pathways are not yet known, although it is possible that the Cph1-Rcp1 phosphorelay network plays a role in red/far-red phototaxis in *Synechocystis* sp. PCC6803 (Choi et al. 1999). It is known that the phosphorylation-induced conformational change of response regulators serves as switching function. To better understand the light regulation mechanism of cyanobacteria, we determined the 1.9 Å crystal structure of Rcp1 using the multiwavelength anomalous dispersion method. As expected, its overall structure is similar to those of the corresponding domains of other response regulators; however, conformations of conserved residues related to phosphorylation relay do not coincide with the structures of other unphosphorylated response regulators. Here, we describe the structure of unphosphorylated Rcp1, compare it with those of phosphorylated and unphosphorylated CheY and FixJN, and discuss the structure terms of its implications for phosphorylation-induced conformational changes and signaling.

Results

Tertiary structure of Rcp1

The crystal structure of Rcp1 from *Synechocystis* sp. PCC6803 was solved using the multiple wavelength anomalous dispersion method with a selenomethionine derivative, and the model was refined to a resolution of 1.9 Å. The structure, illustrated in Figure 1a, is a single domain protein consisting of 147 residues that folds into a $(\beta/\alpha)5$ topology, with five β-strands forming the hydrophobic core, sandwiched between two helices on one side and three helices on the other. The strands and helices alternate along the primary structure with a topology of β2-β1-β3-β4-β5, and are tightly connected by turns and short loops. Sequence alignment of Rcp1 with other response regulators having known structures shows a high degree of conservation among their receiver modules (Fig. 1b). The fold of Rcp1 is similar to the bacterial chemotaxis receiver domain of CheY, which shows 19% overall sequence identity with the 147 residues of Rcp1. In both structures, the C_α atom pairs of the five structurally conserved β-strands in the core can be superimposed with a root mean square deviation (RMSD) of 0.71 Å.

On the other hand, helix α5 and loops L2 and L4 contribute to major conformational differences between Rcp1 and CheY (Fig. 2a). L4, the longest loop, comprised of the 13 residues from Glu51 to Asn63, contains seven residues absent from other response regulators and contains one turn of α-helix at the protruding end. Helix α5 is positioned differently from that in CheY and the other response regulators. This is because in Rcp1 the neighbor of Lys120 is a serine instead of a proline, as in other response regulators. As a consequence, Ser121 adds one residue to the β5 strand and contributes to the displacement and rotation of loop L9 and helix α5 (Fig. 2b). The helix α5 of Rcp1 contains one additional turn of helix than CheY, is tilted by 20°, and is shifted toward the N-terminus along the helical axis.

Rcp1 forms a dimer

The Rcp1 monomer was initially purified and crystallized using 3.2 M ammonium sulfate as the precipitant. Within the crystal, however, Rcp1 is a tightly associated dimer, and the respective monomers (designated molecules A and B) are related by a noncrystallographic two-fold symmetry axis (Fig. 2c). The surface area buried upon dimer formation is 1161 $Å^2$ or 15% of the total surface area of each monomer. The dimer interface consists of loop L6, loop L8, β5, α4, and the C-terminus of α5. A group of hydrophobic side chains along the surface of the C-terminal half of the domain pack onto what would otherwise be an extensive exposed hydrophobic patch on the partner subunit. The Phe137 and Trp138 residues from each monomer are packed closely around the twofold axis of the interface, and at the center of the interface, Phe137, Trp138, Val142, Leu118, and Ile134 compose the hydrophobic patch of each monomer and interact by hydrophobic forces. In addition, 11 hydrogen bonds and two salt bridges around the hydrophobic interface link the monomers. Consequently, the C-terminal portion consisting of α4, β5, and α5 forms a dimer interface that is highly susceptible to phosphorylation induced conformational changes. The RMSD for all C_α atoms between the protomers is 0.787 Å, and the major structural differences arise from loops L4 and L9. The different conformations in loops L4 might be due to different crystal packing environments, as the structure of Rcp1 crystallized under the same conditions but with a different space group ($P6_3$) showed the same dimeric interactions and has a RMSD of 0.88 Å with the structure of a $P2_1$ space group form for all backbone atoms of the dimer. The crystal structure of $P6_3$ space group also has similar active site geometries

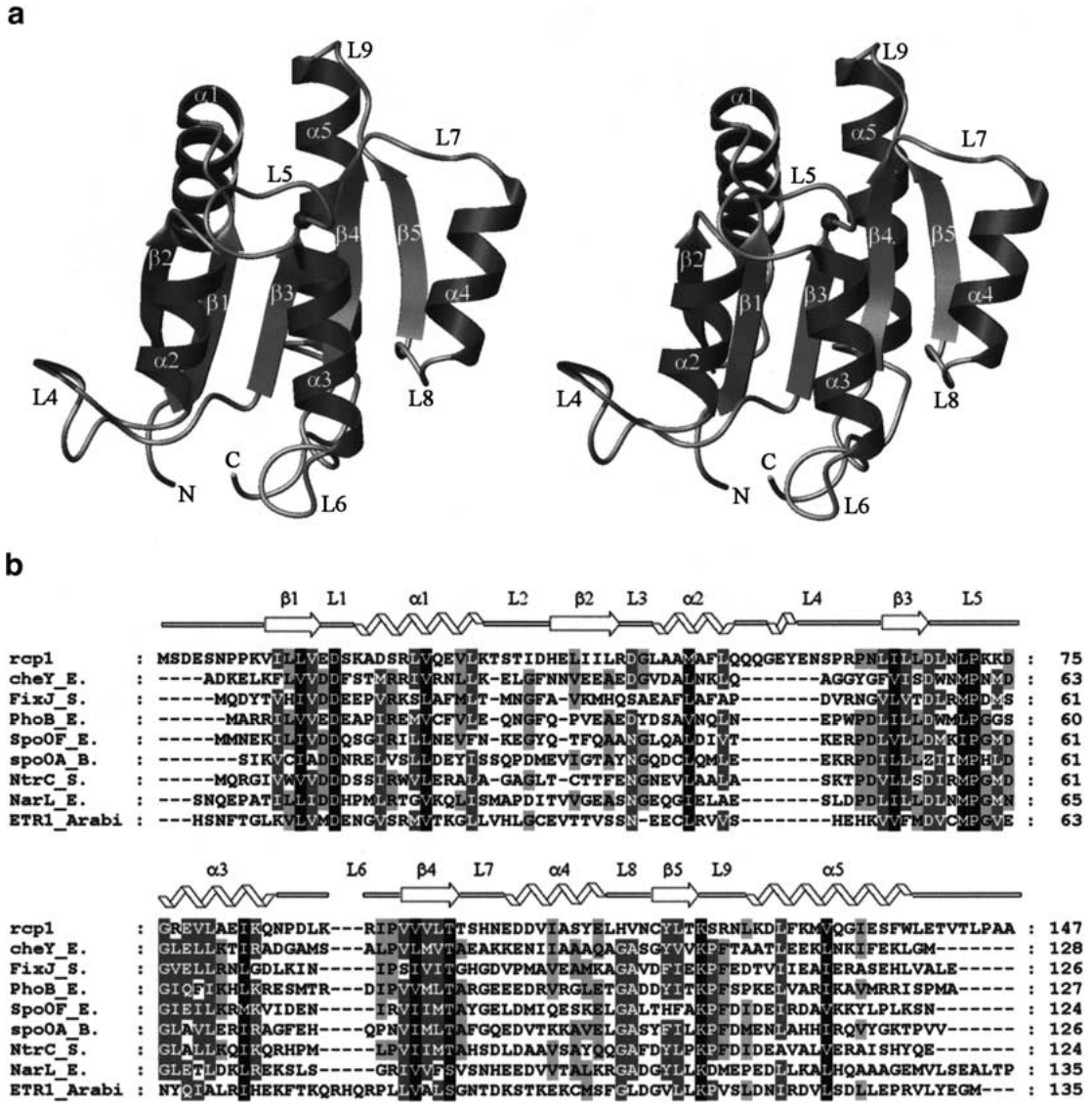

Fig. 1. Structure of Rcp1. (*a*) Ribbon representation of the Rcp1 monomer. The order of the β strands and α helices is indicated; the black sphere indicates the position of the Asp68. (*b*) Sequence alignment of response regulators for which the structures of the receiver domains are known. Highly conserved residues are shaded black; similar residues are shaded gray. Sequence alignment was done using *ClustalX* (Thompson et al. 1997). The structures represented are *Synechocystis* sp. Rcp1 (this work), *E. coli.* CheY (Volz and Matsumura 1991; Stock et al. 1993), *S. meliloti* FixJN (Birck et al. 1999), *E. coli* PhoB (Sola et al. 1999), *Bacillus sbtilis* Spo0F (Feher et al. 1995), *Bacillus sbtilis* Spo0A (Lewis et al. 1999), *Salmonella typhimurium* NtrC (Volkman et al. 1995), *E. coli* NarL (Baikalov et al. 1996) and *Arabidopsis thaliana* ETR_{RD} (Muller-Dieckmann et al. 1999).

and conformations with the activated form of response regulators.

Active site

The active site of Rcp1 is located in a crevice formed by loops L1 and L5, as occurs in other response regulators, and all receiver domains include four highly conserved residues: Glu15, Asp16, Asp68, and Lys120 (Asp12, Asp13, Asp57, and Lys109 in CheY). Glu15, Asp16, and phosphate-accepting Asp68 form an acidic pocket (Fig. 3a). Lys120 from L9 points into the acidic pocket at the three carboxylate side chains of Glu15, Asp20, and Asp68. The $O^{\delta 1}$ of the carboxylate side chain of Asp68 is hydrogen bonded to Lys120, and interestingly, the $O^{\delta 2}$ of Asp68 is hydrogen bonding directly with the side chain oxygen of Thr98 over a distance of 2.9 Å.

W1, located at the end of side chain of Asp68 in molecule A, hydrogen bonds with the side chain of Thr98 and bridges the hydrogen bonds between the Asp86 and a sulfate ion. In

Table 1. *Data collection and phasing and refinement statistics*

Data set	Se (Apo-Rcpl)			Mn-Rcp1
Wavelength (Å)	λ1	λ2	λ3	
	0.9795	0.9793	0.9500	1.54
Resolution (Å)	15–1.9	15–1.9	15–1.9	50–2.3
Observations	83143	61424	61264	27451
Unique reflections	20025	19386	19380	10745
Data coverage total/final shell (%)[a]	98.5/98.5	98.1/98.1	98.2/98.2	92.0/78.8
R_{merge} total/final shell (%)[b]	4.6/15.5	4.7/15.7	5.2/17.2	4.7/9.6
Phasing (15–1.9 Å)				
Overall figure of merit	0.69 (SOLVE)			
Refinement		Apo-Rcpl		Mn–Rcpl
Resolution (Å)		15–1.9		50–2.3
R_{cryst}[c] total (%)		18.8		22.5
R_{free}[d] total (%)		22.2		28.5
Number of protein, nonhydrogen atoms		2258		2235
Number of solvent atoms		269		143
R.m.s. bond length (Å)		0.005		0.008
R.m.s. bond angle (°)		1.2		1.3
Average B value (Å^2)		14.5		23.5
Main chain		12.2		22.7
Side chain		17.0		24.4

[a] The highest resolution shell for Rcpl was 2.0–1.9 Å.
[b] $R_{merge} = \sum | <I> - 1 / \sum <I>$.
[c] $R_{cryst} = \sum | |Fo| - |Fc| | / \sum |Fo|$.
[d] R_{free} calculated with 10% of all reflections excluded from refinement stages using high-resolution data.

addition, Thr98 is hydrogen bonded to the side chain amides of Asn70 and W1. It is well known that upon phosphorylation of the regulatory domain, the side chain of the conserved Ser/Thr in β4 reorients to within hydrogen bonding distance of the phosphoryl group oxygen (Robinson et al. 2000). Phosphorylation induces movement of backbone residues 98–112 in Rcp1 as well as reorientation of the Thr98 side chain. In this crystal structure, Thr98, whose hydroxyl forms a contact with the carboxyl group of Asp68, thus proceeds toward Asp68 in the absence of phosphorylation.

The active sites of molecules A and B each contain a sulfate ion and several water molecules (Fig. 3a). A water molecule (W2) at the Mg^{2+} site in Apo-Rcp1 hydrogen bonds with the carboxylic side chains of Asp15, Glu16, and Asp68. The sulfate ions originated from the crystallization solution, and were centrally located in the accessible regions of the active sites, where oxygen atoms are close to the N^{ε} of Lys120, N^{δ} of Asn70, and four water molecules. In the vicinity of the active site of molecule A, side chains of His101 and Asn102 form a symmetry-related molecule located over the active pocket. The side chains of these residues stabilize the sulfate ion through hydrogen bonds of 2.9 and 3.3 Å, respectively. The sulfate ion present under crystallization conditions often binds to the phosphorylation site, as several crystal structures of unphosphorylated CheY containing a sulfate ion in the active site have been reported (Volz and Matsumura 1991; Kato et al. 1998). The sulfate ion is located at the site where the phosphoryl group might be placed when phosphorylated histidine kinase recognizes the active site. The existence of a sulfate ion in the active site does not imply the structure resembles the phosphorylated form, however.

To determine the structure coordinating the metal ion, the crystal was soaked in a crystallization solution containing 10 mM $MnCl_2$, and the structure of Mn-Rcp1 was solved using the Apo-Rcp1 structure as a model (Fig. 3b). Within the Mn^{2+} bound structure of Rcp1, the metal ion shows a strong electron density at the active site of molecule A in the anomalous difference electron density map (6.8 σ) and the omit map (14 σ). The Mn^{2+} is located at the site of a water molecule in the apo-Rcp1, and its coordination sphere consists of the carboxylate oxygens of Asp16 and Asp68, the backbone carbonyl oxygen of Asn70, a water molecule (W3), and two sulfate oxygen atoms. The binding of Mn^{2+} induces small conformational changes in the active site residues, as the side chains of Asp16 and Asp68 form salt bridges with the metal ion. The position of the sulfate ion is shifted 1.1 Å toward Asp68, compared to apo-Rcp1, and the two sulfate oxygens interact with the Mn^{2+}. The side chains of His101 and those of Asn102 and Ser100 of the neighboring molecule, which hydrogen bond with the sulfate ion in apo-Rcp1, turn away from the sulfate ion in the metal-bound structure. Interestingly, although the active sites of molecules A and B both contain a sulfate ion, and molecule B is more exposed to solvent, only molecule A contains a

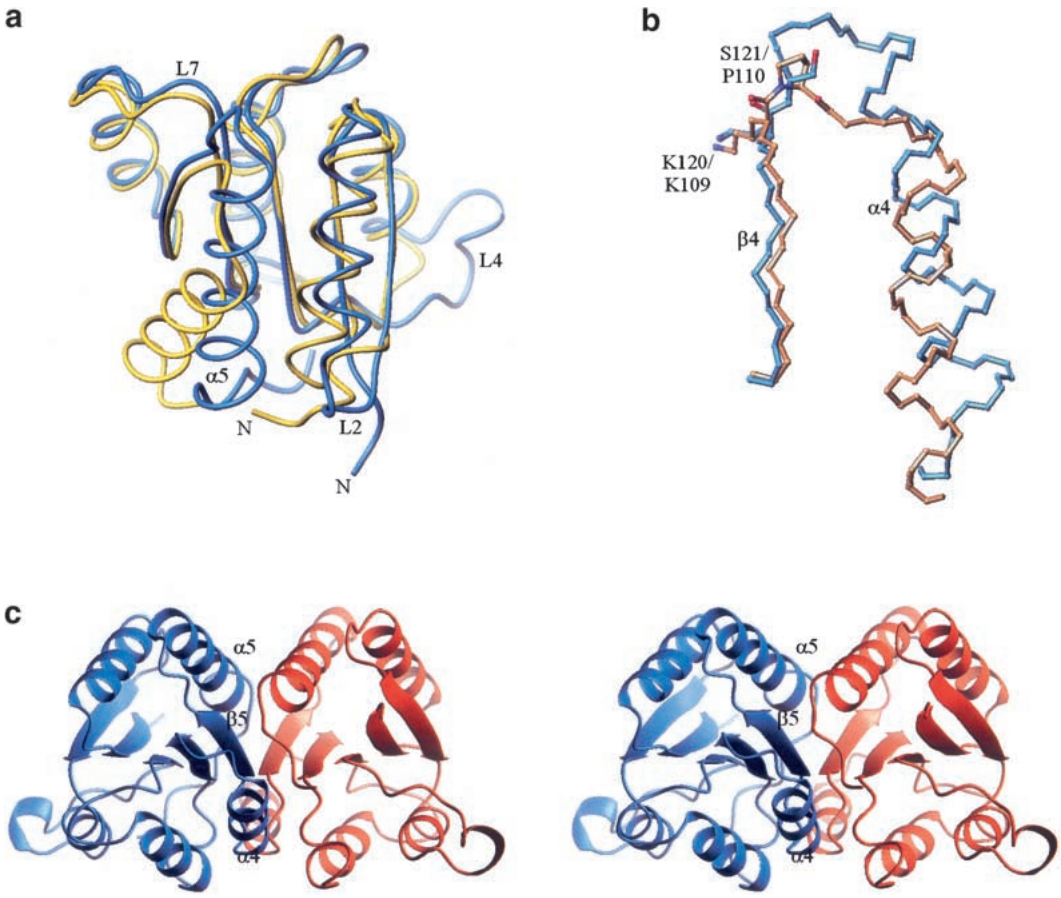

Fig. 2. (*a*) Superposition of Rcp1 (blue) and CheY (yellow, PDB id 3chy; Volz and Matsumura 1991). The structurally well-conserved five-stranded β core was used for structure superposition. (*b*) Superposition of the backbone structures of β5 and α5 of Rcp1 (blue) and CheY (orange). The side chains of Ser121 in Rcp1 and Pro110 in CheY are shown for clarity. (*c*) Stereoview of the Rcp1 dimer. Molecule A is shown in blue and molecule B in red. The three secondary structures participating in the dimer interface are indicated.

metal ion. In molecule B, Lys120 from β5 forms a close salt bridge with the side chains of Glu15 and Asp68, thereby creating an unfavorable environment for metal binding. It seems that the high ionic strength in the solution and the subtle different conformation of the side chains in the active sites result in asymmetric binding of Mn^{2+} in the dimer. The C_α RMSD between the Mn-Rcp1 and the apo-Rcp1 is 0.802 Å. However, hydrogen bonding between Asp68 and Thr98 is maintained in all protomers of metal-bound and metal-free Rcp1 structures. Aside from the conformation of the residues coordinating the metal ion, little difference was observed between the two structures.

Conformational changes upon phosphorylation

The outstanding question regarding response regulators is the nature of the conformational change upon phosphorylation that underlies the switching mechanism. Activated structures of several response regulators, CheY (Lee et al. 2001), FixJ (Birck et al. 1999), and Spo0F (Lewis et al. 1999) were reported. Phosphorylation of a converved aspartate at the active site mediates a conformational change providing a structural relay between the phosphorylation site and a conserved aromatic residue on the distal face of the domain. To address the question concerning Rcp1, we have compared the structures with other response regulators whose activated and unphosphorylated structures were reported. Figure 4 shows our comparison of the geometries of the side chains of Thr98 and Tyr117, which are known to undergo conformational changes upon activation. Five conserved core β-strands were used for superposition of the structures. In CheY, the side chain of the conserved Thr in β4 reorients for hydrogen bonding to the phosphoryl oxygen atom at the active site. The side chain of the conserved Tyr residue, located in the surface of the protein defined by β5, rotates inward, toward the site of phosphorylation, filling the cavity vacated by the repositioned Thr residue.

We found that the crystal structure of unphosphorylated Rcp1 is similar to the activated forms of other response regulators. The side chains of Thr98 and Tyr117 adopt in-

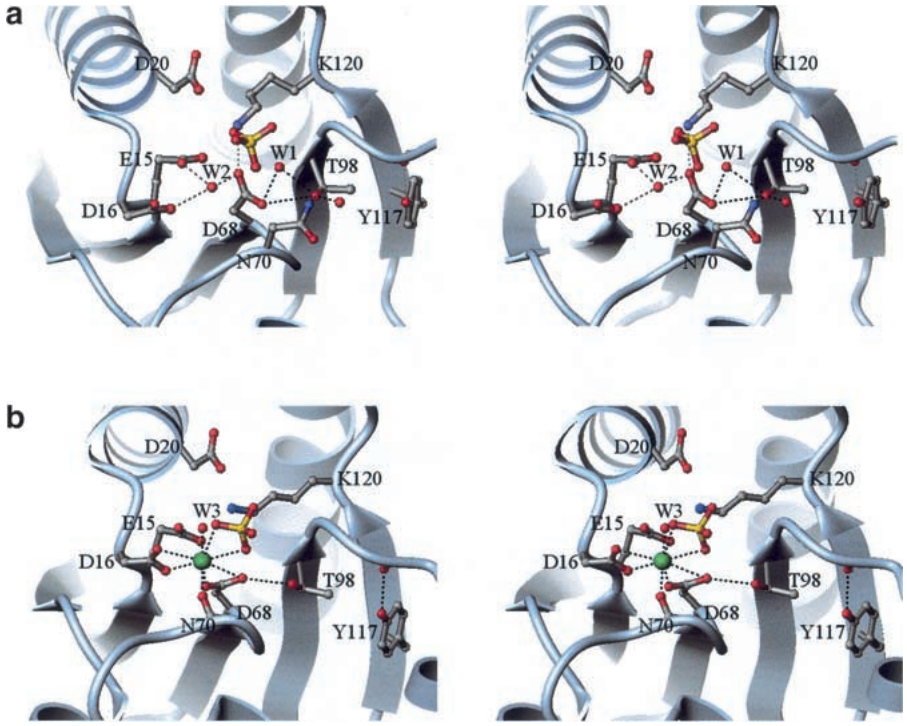

Fig. 3. Stereoview of the Rcp1 active site. (*a*) Active site in molecule A of the apo-Rcp1 structure. All interactions depicted by dashed lines are between 2.5 and 3.5 Å. (*b*) Active site in molecule A of the Mn-Rcp1 structure. Mn^{2+} is shown as a green sphere.

ward positions, and Thr98 in Rcp1 hydrogen bonds with the side chain oxygen of active site residue Asp68. Thr98 is in an inward position making a 2.9 Å hydrogen bond directly with the side chain oxygen of unphosphorylated Asp68 and a water molecule located in the active site. The distance between the C_α atoms of Asp68 and Thr98 in Rcp1 is 4.70 Å, which is closer to the distance of the activated form of CheY (4.87 Å) than the unphosphorylated form (5.85 Å). Tyr117 is also in an inward position, hydrogen bonding with the backbone carbonyl oxygen of Ser100, which yields in a conformation very close to that of activated CheY (Fig. 4a). The outward location of the Tyr117 side chain within the dimer structure is unfavorable due to the steric requirement at the dimer interface. Likewise, the conformation of loop L7, connecting β4 and α4, and the relative orientation of helix α5, which undergo major structural changes upon activation, are also close to the activated structure of CheY.

We also compared the structure of unphosphorylated Rcp1 with the FixJ regulator domain (FixJN) whose phosphorylated and unphosphorylated structures are known (Fig. 4b). Superposition of phosphorylated and unphosphorylated FixJN shows that phosphorylation-induced conformational changes occur in loop L5, connecting β3-α3, in loop L7, connecting β4-α4, and in helix α4. To determine whether or not the crystal structure of Rcp1 is close to that of phosphorylated FixJN, four structurally conserved core β-strands, which do not undergo phosphorylation induced conformational changes, were used to superimpose the three structures. It is obvious that in all three aforementioned regions undergoing structural changes upon phosphorylation in FixJN, the structure of the Rcp1 more closely superimposes the phosphorylated form of FixJN than the unphosphorylated form; RMSD for the 22 residues undergoing phosphorylation-induced conformational changes in FixJN is 1.86 Å for phosphorylated FixJN and Rcp1, and 3.21 Å for unphosphorylated FixJN and Rcp1. The structure of the unphosphorylated Rcp1 dimer is thus more similar to the structure of phosphorylated FixJN.

Discussion

The crystal structure of unphosphorylated Rcp1 is similar to the activated forms of other response regulators. This unexpected findings described here highlight a possible conflict between the phosphorylated and unphosphorylated structures of Rcp1. Therefore, we attempted to solve the phosphorylated structure of Rcp1. A functional study in which Rcp1 monomers were phosphorylated using the small phospho-donor acetylphosphate produces a dimer fraction, as identified by a size-exclusion chromatographic column, suggesting that, in vitro, Rcp1 is a monomer that forms a dimer upon phosphorylation (Fig. 5). However, obtaining a large amount of phosphorylated protein suitable for a crystallization trial was not possible due to the instability of

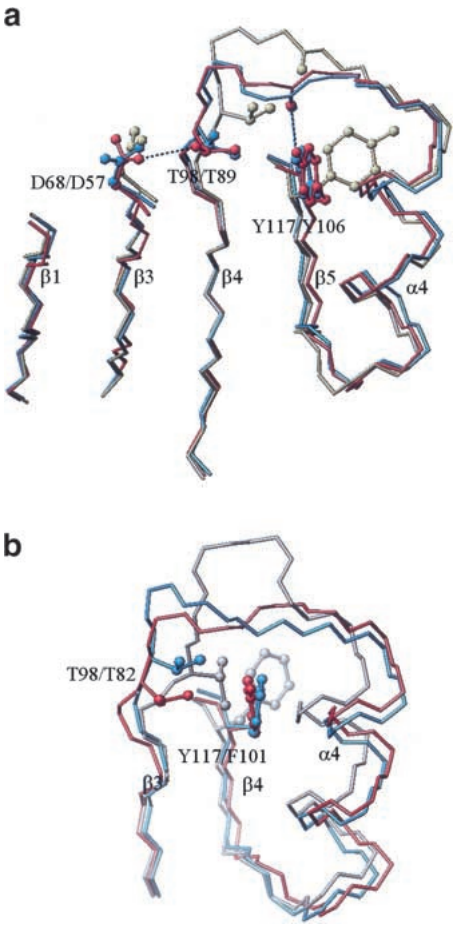

Fig. 4. (*a*) Superposition of the backbone structures of Rcp1 (red; this work), CheY (ivory, PDB id 3chy; Volz and Matsumura 1991), and BF_3^--activated CheY (blue, PDB id 1f4v; Lee et al. 2001). Five structurally conserved core β-strands were used for superposition. Side chains of key residues involved in activation relay are shown. (*b*) Superposition of the backbone structures of Rcp1 (red; this work), FixJN (ivory, PDB id 1dbw; Birck et al. 1999) and phosphorylated FixJN (blue, PDB id 1d5w; Birck et al. 1999).

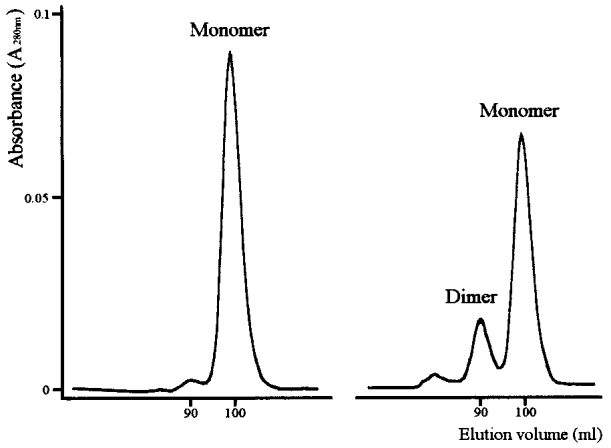

Fig. 5. Size-exclusion chromatography profiles of unphosphorylated Rcp1 (*left*) and phosphorylated Rcp1 (*right*). Purified monomer rcp1 was phosphorylated by incubating 0.1–0.2 mM pure Rcp1 monomer with 30 mM acetyl phosphate in 20 mM Tris-HCl (pH7.5), 10 mM $MgCl_2$ for 3 h at room temperature. EDTA (10 mM) was then added to the mixture. The dimer was identified using superdex 200 (HiLoad 16/60) size-exclusion chromatographic column.

phosphorylated form. Interestingly, although only monomers were used, unphosphorylated Rcp1 crystallized as a dimer, yielding a conformation very similar to that of phosphorylated CheY. We suppose that this dimerization was induced by the high ionic strength (3.2 M $[NH_4]_2SO_4$) in the crystallization buffer, as unphosphorylated Rcp1 contains hydrophobic patches at the dimer interface. A group of hydrophobic residues along the surface of the C-terminal half of a domain composing dimer interface pack onto what would otherwise be an extensive exposed hydrophobic patch on the partner subunit. Indeed, even if we assume that the crystal structure of Rcp1 is an artifact of the crystallization condition, it can nevertheless serve as a model enabling inference of much about the structure of the phosphorylated dimer, and therefore, make reasonable deductions regarding the conformational changes resulting from phosphorylation.

Based on comparisons with the structures of other response regulators, it appears that the crystal structure of the unphosphorylated Rcp1 dimer mimics the phosphorylated structure in several ways: (1) hydrogen bonding between the phosphate and the threonine residue corresponds to the direct hydrogen bonding between the carboxylic oxygen of Asp68 and the side chain of Thr98. In all other unphosphorylated response regulators known there is no direct hydrogen bonding between an active site residue and the threonine residue. (2) The inward conformation of Thr98, which is pulled toward Asp68, is close to the phosphorylated structure of other response regulators. (3) The conformation of the loop connecting β4 and α4 and the orientation of helix α4, which undergoes major structural changes upon phosphorylation, are very similar to those of phosphorylated response regulators. Loop L7 contains several flexible residues, as indicated by the high temperature factors (Fig. 6c), and because this area is connected to the active site, hydrogen bonding of the threonine with the phosphoryl group can easily trigger large changes in its conformation. In addition, Thr98 is at the interface between helix α4 and the β-sheet core of the protein, and its movement can alter the β4α4 loop and the N-terminus of helix α4. (4) Inward aromatic switching of Tyr117 is also conserved in the crystal structure of Rcp1. The hydroxyl group of Tyr117, which hydrogen bonds with the backbone carbonyl oxygen of Ser100 in the loop L7, stabilizes these conformations, as is reported for the structure of CheY complexed with the phosphoryl group mimic beryllofluoride (Lee et al. 2001). In the context of these features, it seems reasonable to conclude that the crystal structure of Rcp1 is similar to the phosphorylated structure of Rcp1. It is probable that the concerted move-

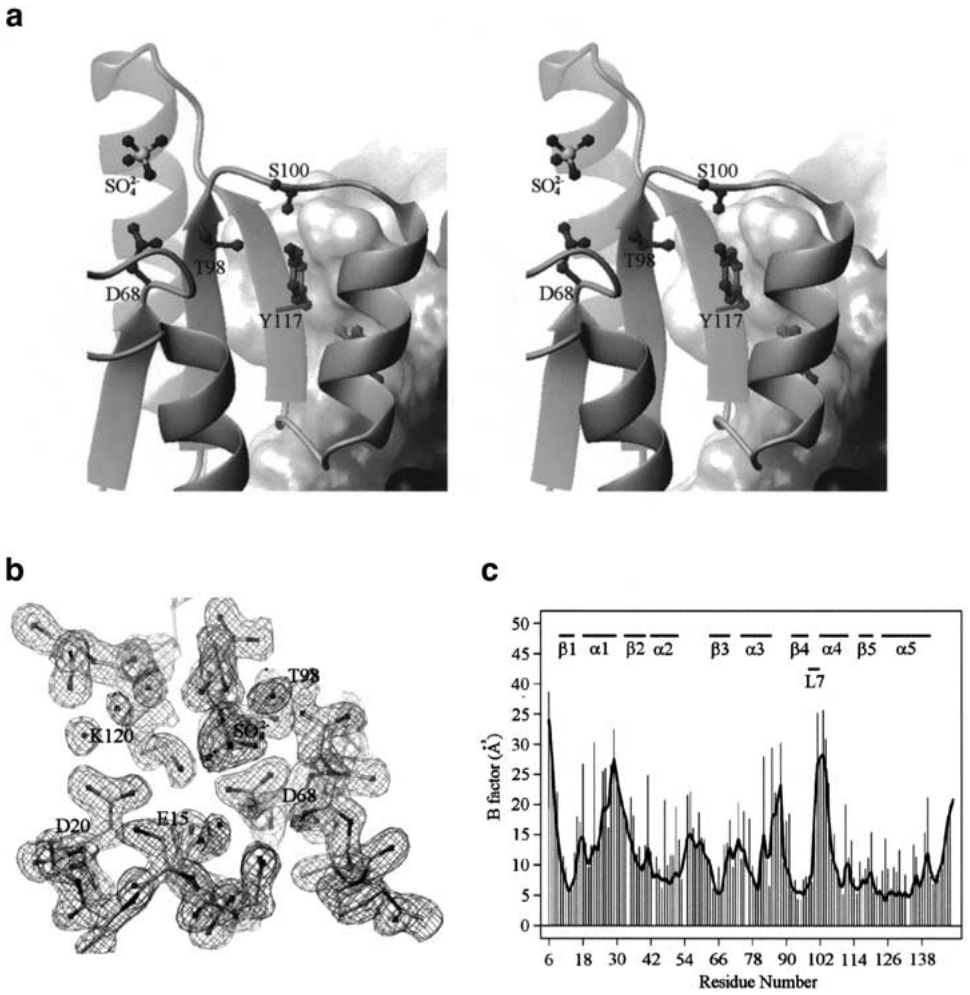

Fig. 6. (*a*) Stereoview of the ribbon representation of the conserved side chains of Rcp1. The surface of molecule B is shown. (*b*) $2F_o - F_c$ electron density map at 1.9 Å, contoured at 1 σ around the active site with the final refined model superimposed. (*c*) Average temperature factor versus residue number for Rcp1. Schematic of the secondary structure elements is included.

ments of residues in unphosphorylated Rcp1 originate from the high ionic strength in the crystallization buffer. Because of the aforementioned exposed hydrophobic patch, the monomeric state of Rcp1 would be unfavorable in a high salt environment, and dimerization would be expected to occur spontaneously. The dynamic nature of the conformational changes in the response regulator would allow dimerization, stabilizing the active conformation and resulting in the reverse movement of residues involved in the activation relay. Inward rotation of Tyr117 is required for dimerization to avoid steric hindrance at the dimer interface, and subsequent inward movement of Thr98 should occur to accommodate the bulky tyrosine residue. Flexible loop L7, which changes its conformation to the activated form, is stabilized by newly formed hydrogen bonds between the hydroxyl group of the rotated tyrosine residue and the backbone carbonyl oxygen of loop L7. The position of Thr98 at the base of loop L7 shifts, enabling it to hydrogen bond with the active site residue Asp68.

This raises a key question: is the crystal structure of this high ionic strength-induced dimer the same as the phosphorylation-induced dimer in solution? It is unlikely that the conformation of the unphosphorylated crystal structure of Rcp1 is exactly the same as that of phosphorylated Rcp1, because the effect of hydrogen bonding between phosphate and Thr98 would differ from that of direct hydrogen bonding of Asp68 with Thr98. However, the overall structure of phosphorylated Rcp1 would be very similar to this crystal structure, because the principle requirements for the activation are satisfied by the hydrogen bonding of Asp68 with Thr98 and the conformational changes of the other residues involved in activation.

The Rcp1 dimer interface consists of residues in α4, β5, and α5, a region that shows large phosphorylation-induced structural changes in other response regulators. Tyr117 of helix α4 participates in dimer interaction with β5 and α5 (Fig. 6a), and corresponds to Tyr106 of CheY, which is involved in signal transduction (Schuster et al. 2000). The

inward/outward positioning of the Tyr106 side chain is modulated by the phosphorylation state of CheY (Zhu et al. 1996). Tyr117 of Rcp1 may have a similar signaling function, because the inward movement of the side chain is required for dimerization. This residue belongs to the C-terminal surface of the receiver domain, which is most affected by the phosphorylation-induced structural changes and is frequently referred to as the "signaling surface" of response regulators (Zhu et al. 1997).

The conformational change in the C-terminal half of the domain in CheY upon phosphorylation increases the affinity of CheY to a flagella switch protein FliM, resulting in altered movement of flagellum (Falke et al. 1997; Djordjevic and Stock 1998). In some response regulators having additional C-terminal DNA binding domain such as Spo0A, FixJ, PhoB, NtrC, dimerize upon phosphorylation with the dimer interfaces composed of C-terminal regions of regulatory domains (Asayama et al. 1995; Fiedler and Weiss 1995; Da Re et al. 1999). Dimer form of the response regulator then binds to DNA and serves as a transcription factor. A large part of the dimer interface of Rcp1 coincides with the phosphorylation-dependent interface of CheY. The regions altered by phosphorylation coincide with the surfaces that participate in protein–protein interactions regulated by phosphorylation, suggesting the dimerization of Rcp1 is involved in its regulatory function. Rcp1 may thus function as a phosphotransferase or may have distinct regulatory activities as does CheY.

Conclusions

Photosynthetic organisms from bacteria to higher plants possess a variety of light-sensing molecules, enabling detection of light and adaptation to fluctuations in intensity, direction, duration, polarization, and spectral quality (Kendrick and Kronberg 1994). Cph1 and Rcp1 comprise a two-component light signaling system modulated by red and far-red light (Yeh et al. 1997). The signal transduction pathway downstream of Rcp1 is not yet known, although it is known that the phosphate receiver domains are conserved in all members of the response regulator superfamily, and that their phosphorylation state controls the function of the output domains or the regulatory domain itself. And like CheY, the two forms of the small receiver molecule, Rcp1 and phospho-Rcp1, may have distinct regulatory activities. The three-dimensional structure of Rcp1 exhibits the conserved doubly wound five-stranded α/β fold of receiver domains and an active site similar to that of CheY. Rcp1 lacks an effecter domain; however, the monomer-dimer state is phosphorylation dependent. The regulation of phosphorylation-dependent dimerization may be mediated by the reorientation of the conserved Tyr117 residue. A large part of the dimer interface of Rcp1 coincides with the phosphorylation-dependent interface of other response regulators and contains conserved residues that undergo conformational changes upon phosphorylation. If the phosphorylation-dependent interface is conserved in Rcp1, its dimerization could change the properties of the interaction between Rcp1 and downstream target molecules.

Materials and methods

Protein purification and crystallization

Rcp1 was overexpressed in *E. coli* strain B834(DE3) in minimal media containing selenomethionine and purified by IMPACT^R chromatography as described previously (Im et al. 2000). Crystals of Rcp1 were grown using the hanging drop vapor diffusion method at 294 ± 1 K using a precipitant solution containing 100 mM Tris-HCl (pH 8.5) and 3.1 M ammonium sulfate. Under the same crystallization conditions, crystals were grown by microseeding with or without subsequent macroseeding to increase the size of crystals. This yielded crystals belonging to space groups $P6_3$ and $P2_1$, respectively. The unit cell dimensions of the hexagonal crystals were a = b = 89.0 Å, c = 60.3 Å, and there were two molecules in the asymmetric unit. The monoclinic crystal also contained two molecules in an asymmetric unit with unit cell dimensions a = 41.4 Å, b = 77.0 Å, c = 43.0 Å, and β = 106.2°. Because the monoclinic form crystal diffracts better, this crystal form was used for MAD experiments.

Data collection and processing

Crystals were directly transferred to Paratone-N (Hampton Research) and flash cooled at 100 K for data collection. The MAD data was collected at Beam line BL18B at the Photon Factory in Japan using an ADSC Quantum-4 CCD detector. Diffraction images were processed using the MOSFLM program suite (Leslie 1994), and the structural factors were scaled and reduced using the SCALA program from the CCP4 package (CCP4 1994). The selenomethionine positions were located using the program SOLVE (Terwilliger and Berendzen 1997) while treating the data as a special case of multiple isomorphous replacements with anomalous scattering, and by using the remote wavelength data set as a pseudo-native data set. The initial phase was calculated using the program SHARP (La Fortelle 1997), with heavy atom positions obtained with SOLVE. Solvent flattening and histogram matching, as implemented in the program DM (CCP4 1994; Cowtan 1994), further improved the phases, with a figure of merit 0.83. For Mn^{2+} derivatization, crystals were soaked in reservoir solution containing 10 mM $MnCl_2$ for 24 h. The data was collected on an R-AXIS IV image plate system attached to a Rigaku rotating-anode generator (RU 300) providing CuK_α radiation and running at 50 kV and 90 mA with a 0.3 mm focus cup in a nitrogen–gas stream at 110 K (Oxford Cryosystem). The data were indexed and processed using DENZO and SCALEPACK (Otwinowski and Minor 1997). To determine the structure of Mn^{2+}-bound Rcp1, molecular replacement calculations were carried out with AMoRe (Navaza 1994) using the native Rcp1 dimer model solved by the MAD method. The model was built using the program O (Jones et al. 1991), and refinement was done using the program CNS (Brünger et al. 1998). Structure of the hexagonal crystal form was solved at 2.5 Å resolution by molecular replacement using the $P2_1$ crystal structure. The structure was refined to the R_{factor} of 25.4% and R_{free} of 32.3 %, which has the same active site stereochemistry and dimeric interaction with Cα RMSD of 0.88 Å (data not shown).

Model building and refinement

The MAD phased, solvent flattened electron density map calculated to a 1.9 Å resolution showed good electron density for all the residues except for some side chains in the loop regions. This map allowed excellent tracing of the residues using O. Once molecule A was built, it was copied to the rest of the density using NCS parameters. In the early stage of refinement, energy minimization, simulated annealing and B-factor refinement were carried out using CNS without NCS restraints. Ambiguous residues in the initial map were then introduced into the model and refinement was continued employing addition of water molecules. The final working R_{factor} was 18.8% (R_{free} 22.2%). The N-terminal six residues from molecule A, N-terminal seven residues from molecule B and C-terminal two residues from molecule B were disordered and were not modeled. A Ramachandran plot generated with the program PROCHECK (Laskowski et al. 1993) shows the current model to exhibit good geometry with 93.3% of the residues in the most favored regions, 5.9% of the residues in additional allowed regions, and one residue, Lys73, in a disallowed region. This residue, however, is involved in a classical γ-turn and is well defined both in the experimentally phased and in the refined electron density maps. Figures were prepared with MOLMOL (Koradi et al. 1996).

Structure superposition and alignments

The structure of CheY was superimposed on that of Rcp1 using the program O. We determined this set by choosing the atoms from the structurally well conserved five core β-strands. Superposition of Rcp1, FixJN, and phosphorylated FixJN was done using the four structurally conserved β-strands that do not undergo phosphorylation-induced structural changes: residues 11–14, 64–67, 93–97, and 116–119 in Rcp1, and residues 6–9, 50–53, 77–81, and 100–103 in FixJN.

Accession numbers

The atomic coordinates and the structural factors of Apo-Rcp1 and Mn-Rcp1 have been deposited with the Protein Data Bank of the Research Collaboratory for Structural Bioinformatics (RCSB) with the accession codes 1I3C and 1JLK.

Acknowledgments

We thank Prof. Noriyoshi Sakabe, Drs. M. Suzuki, and D. N. Igarashi of Beamline BL18B at Photon Factory, Tsukuba, Japan, for their generous support during crystallographic data collection. We also thank Prof. Se Won Suh for supporting the data processing. This work was supported in part by grants from NIH (GM-36956 to Song), BK21, NRL (2000-N-NL-01-C-063 to Song), KRF (to Park), and Critical technology 21.

The publication costs of this article were defrayed in part by payment of page charges. This article must therefore be hereby marked "advertisement" in accordance with 18 USC section 1734 solely to indicate this fact.

References

Alex, L.A., Borkovich, K.A., and Simon, M.I. 1996. Hyphal development in *Neurospora crassa*: Involvement of a two-component histidine kinase. *Proc. Natl. Acad. Sci.* **93:** 3416–3421.

Asayama, M., Yamamoto, A., and Kobayashi, Y. 1995. Dimer formation of phosphorylated Spo0A, a transcriptional regulator, stimulates the *spo0F* transcription at the initiation of sporulation in *Bacillus subtilis*. *J. Mol. Biol.* **250:** 11–23.

Baikalov, I., Schroder, I., Kaczor-Grzeskowiak, M., Grzeskowiak, K., Gunsalus, R.P., and Dickerson, R.E. 1996. Structure of the *Escherichia coli* response regulator NarL. *Biochemistry* **35:** 11053–11061.

Birck, C., Mourey, L., Gouet, P., Fabry, B., Schumacher, J., Rousseau, P., Kahn, D., and Samama, J. P. 1999. Conformational changes induced by phosphorylation of the FixJ receiver domain. *Struct. Fold. Des.* **7:** 1505–1515.

Brünger, A.T., Adams, P.D., Clore, G.M., DeLano, W.L., Gros, P., Grosse-Kunstleve, R.W., Jiang, J.-S., Kuszewski, J., Nilges, M., Pannu, N.S., Read, R.J., Rice, L.M., Simonson, T., and Warren, G.L. 1998. Crystallography & NMR system: A new software suite for macromolecular structure determination. *Acta Crystallogr. D* **54:** 905–921.

Chang, C., Kwok, S.F., Bleecker, A.B., and Meyerowitz, E.M. 1993. *Arabidopsis* ethylene-response gene ETR1: Similarity of product to two-component regulators. *Science* **262:** 539–544.

Choi, J.S., Chung, Y.H., Moon, Y.J., Kim, C., Watanabe, M., Song, P.-S., Joe, C.O., Bogorad, L., and Park, Y.M. 1999. Photomovement of the gliding cyanobacterium *Synechocystis* sp. PCC 6803. *Photochem. Photobiol.* **70:** 95–102.

CCP4 (Collaborative Computational Project Number 4). 1994. The CCP4 suite: Programs for protein crystallography. *Acta Crystallogr. D* **50:** 760–776.

Cowtan, K. 1994. "dm": An automated procedure for phase improvement by density modification. *Joint CCP4 and ESF-EACBM Newslett. Protein Crystallogr.* **31:** 34–38

Da Re, S., Schumacher, J., Rousseau, P., Fourment, J., Ebel, C., and Kahn, D. 1999. Phosphorylation-induced dimerisation of the FixJ receiver domain. *Mol. Microbiol.* **34:** 504–511.

Djordjevic, S. and Stock, A.M. 1998. Structural analysis of bacterial chemotaxis proteins: Components of a dynamic signaling system. *J. Struct. Biol.* **124:** 189–200.

Falke, J.J., Bass, R.B., Butler, S.L., Chervitz, S.A., and Danielson, M.A. 1997. The two-component signaling pathway of bacterial chemotaxis: A molecular view of signal transduction by receptors, kinases, and adaptation enzymes. *Annu. Rev. Cell Dev. Biol.* **13:** 457–512.

Feher, V.A., Zapf, J.W., Hoch, J.A., Dahlquist, F.W., Whiteley, J.M., and Cavanagh, J. 1995. ^{1}H, ^{15}N, and ^{13}C backbone chemical shift assignments, secondary structure, and magnesium-binding characteristics of the *Bacillus subtilis* response regulator, Spo0F, determined by heteronuclear high-resolution NMR. *Protein Sci.* **4:** 1801–1814.

Fiedler, U. and Weiss, V. 1995. A common switch in activation of the response regulators NtrC and PhoB: Phosphorylation induces dimerization of the receiver modules. *EMBO J.* **14:** 3696–3705.

Im, Y.J., Park, C.-M., Kim, J.-I., Yang, S.-S., Kang, J.-G., Rho, S.-H., Kim, J.I., Song, W.K., Song, P.-S., and Eom, S.H. 2000. Crystallization and preliminary X-ray crystallographic studies of response regulator for cyanobacterial phytochrome, Rcp1. *Acta Crystallogr. D* **56:** 1446–1448.

Jones, T.A., Zhou, J.Y., Cowan, S.W., and Kjeldgaard, M. 1991. Improved methods for building protein models in electron density maps and the location of errors in these models. *Acta Crystallogr. A* **47:** 100–119.

Kato, M., Mizuno, T., and Hakoshima, T. 1998. Crystallization of a complex between a novel C-terminal transmitter, HPt domain, of the anaerobic sensor kinase ArcB and the chemotaxis response regulator CheY. *Acta Crystallogr. D* **54:** 140–142.

Kendrick, R.E. and Kronberg, G.H.M. 1994. *Photomorphogenesis in plants*, 2nd ed. Kluwer Academic Publishers, Dordrecht, The Netherlands.

Koradi, R., Billeter, M., and Wuthrich, K. 1996. MOLMOL: A program for display and analysis of macromolecular structures. *J. Mol. Graphics* **14:** 51–55.

La Fortelle, E.D., Irwin, J.J., and Bricogne, G. 1997. SHARP: A maximum-likehood heavy-atom parameter refinement and phasing program for the MIR and MAD methods. *Crystallogr. Comput.* **7:** 1–9.

Lamparter, T., Mittmann, F., Gartner, W., Borner, T., Hartmann, E., and Hughes, J. 1997. Characterization of recombinant phytochrome from the cyanobacterium *Synechocystis*. *Proc. Natl. Acad. Sci.* **22:** 11992–11797.

Laskowski, R.A., MacArthur, M.W., Moss, D.S., and Thornton, J.M. 1993. PROCHECK: A program to check the stereochemical quality of protein structures. *J. Appl. Crystallogr.* **26:** 283–291.

Lee, S.Y., Cho, H.S., Pelton, J.G., Yan, D., Henderson, R.K., King, D.S., Huang, L., Kustu, S., Berry, E.A., and Wemmer, D.E. 2001. Crystal structure of an activated response regulator bound to its target. *Nat. Struct. Biol.* **8:** 52–56

Leslie, A.G.W. 1994. *MOSFLM user guide*. MRC-LMB, Cambridge.

Lewis, R.J., Brannigan, J.A., Muchova, K., Barak, I., Wilkinson, A.J. 1999.

Phosphorylated aspartate in the structure of a response regulator protein. *J. Mol. Biol.* **294:** 9–15.
Maeda, T., Wurgler-Murphy, S.M., and Aito, H. 1994. A two-component system that regulates an osmosensing MAP kinase cascade in yeast. *Nature* **369:** 242–245.
Muller-Dieckmann, H.J., Grantz, A.A., and Kim, S.H. 1999. The structure of the signal receiver domain of the *Arabidopsis thaliana* ethylene receptor ETR1. *Struct. Fold. Des.* **7:** 1547–1556.
Navaza, J. 1994. AMoRe: An automated package for molecular replacement. *Acta Crystallogr. A* **50:** 157–163.
Ninfa, A.J. and Magasanik, B. 1986. Covalent modification of the glnG product, NRI, by the glnL product, NRII, regulates the transcription of the glnALG operon in *Escherichia coli*. *Proc. Natl. Acad. Sci.* **83:** 5909–5913.
Ota, I.M. and Varshavsky, A. 1993. A yeast protein similar to bacterial two-component regulators. *Science* **262:** 566–569.
Otwinowski, Z. and Minor, W. 1997. Processing of X-ray diffraction data collected in oscillation mode. *Methods Enzymol.* **276:** 307–326.
Park, C.-M., Kim, J.-Y., Yang, S. -S., Kang, J.-G., Kim, J.-I., Luka, Z., and Song, P.-S. 2000. Chromophore–apoprotein interactions in *Synechocysitis* sp. PCC6803 phytochrome Cph1. *Biochemistry* **39:** 6349–6356.
Parkinson, J.S. 1993. Signal transduction schemes of bacteria. *Cell* **73:** 857–871.
Parkinson, J.S. and Kofoid, E.C. 1992. Communication modules in bacterial signaling proteins. *Annu. Rev. Genet.* **26:** 71–112.
Robinson, V.L., Buckler, D.R. and Stock, A.M. 2000. A tale of two components: A novel kinase and a regulatory switch. *Nat. Struct. Biol.* **7:** 626–633.
Schuster, M., Zhao, R., Bourret, R.B., and Collins, E.J. 2000. Correlated switch binding and signaling in bacterial chemotaxis. *J. Biol. Chem.* **275:** 19752–19758.
Solá, M., Gomis-Ruth, F.X., Serrano, L., Gonzalez, A., and Coll, M. 1999. Three-dimensional crystal structure of the transcription factor PhoB receiver domain. *J. Mol. Biol.* **285:** 675–687.
Stock, A.M., Mottonen, J.M., Stock, J.B., and Schutt, C.E. 1989. Three-dimensional structure of CheY, the response regulator of bacterial chemotaxis. *Nature* **337:** 745–749.
Stock, A.M., Martinez-Hackert, E., Rasmussen, B.F., West, A.H., Stock, J.B., Ringe, D., and Petsko, G.A. 1993. Structure of the Mg^{2+}-bound form of CheY and mechanism of phosphoryl transfer in bacterial chemotaxis. *Biochemistry* **32:** 13375–13380.
Stock, J.B., Ninfa, A.J., and Stock, A.M. 1989. Protein phosphorylation and regulation of adaptive responses in bacteria. *Microbiol. Rev.* **53:** 450–490.
Terwilliger, T.C. and Berendzen, J. 1997. Bayesian correlated MAD phasing. *Acta Crystallogr. D* **53:** 571–579.
Thompson, J.D., Gibson, T.J., Plewniak, F., Jeanmougin, F., and Higgins, D.G. 1997. The ClustalX windows interface: Flexible strategies for multiple sequence alignment aided by quality analysis tools. *Nucleic Acids Res.* **24:** 4876–4882.
Volkman, B.F., Nohaile, M.J., Amy, N.K., Kustu, S., and Wemmer, D.E. 1995. Three-dimensional solution structure of the N-terminal receiver domain of NTRC. *Biochemistry* **34:** 1413–1424.
Volz, K. 1993. Structural conservation in the CheY superfamily. *Biochemistry* **32:** 11741–11753.
Volz, K. and Matsumura, P. 1991. Crystal structure of *Escherichia coli* CheY refined at 1.7 Å resolution. *J. Biol. Chem.* **266:** 15511–15519.
Yeh, K., Wu, S., Murphy, J.T., and Lagarias, J.C. 1997. A cyanobacterial phytochrome two-component light sensory system. *Science* **277:** 1505–1508.
West, A.H. and Stock, A.M. 2001. Histidine kinases and response regulator proteins in two-component signaling systems. *Trends Biochem. Sci.* **26:** 369–376.
Zhu, X., Amsler, C.D., Volz, K., and Matsumura, P. 1996. Tyrosine 106 of CheY plays an important role in chemotaxis signal transduction in *Escherichia coli*. *J. Bacteriol.* **178:** 4208–4215.
Zhu, X., Rebello, J., Matsumura, P., and Volz, K. 1997. Crystal structures of CheY mutants Y106W and T87I/Y106W. CheY activation correlates with movement of residue 106. *J. Biol. Chem.* **272:** 5000–5006.